

Prospective Type Ia Supernova Surveys From Dome A

A. Kim^a, A. Bonissent^b, J. L. Christiansen^c, A. Ealet^b, L. Faccioli^d, L. Gladney^e, G. Kushner^a, E. Linder^d, C. Stoughton^f, L. Wang^{g,h}

^a*Lawrence Berkeley National Laboratory, Berkeley, CA 94720*

^b*Centre de Physique des Particules de Marseille, Marseille, France*

^c*California Polytechnic State University, San Luis Obispo, CA, 93407*

^d*University of California, Berkeley, CA 94720*

^e*University of Pennsylvania, Philadelphia, PA 19104*

^f*Fermi National Accelerator Laboratory, Batavia, IL 60510*

^g*Texas A&M University, College Station, TX 77843*

^h*Chinese Center for Antarctic Astronomy, Nanjing, China*

Abstract

Dome A, the highest plateau in Antarctica, is being developed as a site for an astronomical observatory. The planned telescopes and instrumentation and the unique site characteristics are conducive toward Type Ia supernova surveys for cosmology. A self-contained search and survey over five years can yield a spectro-photometric time series of ~ 1000 $z < 0.08$ supernovae. These can serve to anchor the Hubble diagram and quantify the relationship between luminosities and heterogeneities within the Type Ia supernova class, reducing systematics. Larger aperture ($\gtrsim 4$ -m) telescopes are capable of discovering supernovae shortly after explosion out to $z \sim 3$. These can be fed to space telescopes, and can isolate systematics and extend the redshift range over which we measure the expansion history of the universe.

Keywords: Supernova: Type Ia, Dome A, Surveys, Cosmology

1. Introduction

Dome A, the highest plateau in Antarctica, is being considered as a site for an optical-to-infrared observatory [1, 2]. There are several attributes that make Dome A attractive for Type Ia supernova (SN Ia) observations compared to temperate sites. The boundary layer is at ~ 20 m, above which there is a median optical seeing of $0.3''$ (infrared seeing of $0.2''$). During the long winter night, there are no disruptions over 24 hours due to weather. The atmospheric column density is relatively low. The sky surface brightness in K_{dark} , from $2.27\text{--}2.45$ μm is expected to be at ~ 100 $\mu\text{Jy arcsec}^{-2}$; OH emission drops out in these wavelengths while sky and telescope thermal emission is suppressed compared to temper-

ate sites as is seen at the South Pole [3] and Dome C [4].

Dome A has its disadvantages as well. The long day interrupts the longer-term observations necessary for tracking supernova flux evolution. The polar latitude limits the area of sky accessible by a telescope. Auroral activity produces high UV to B band sky emission with non-uniform spatial structure. There are technical hurdles as well, including the remoteness of the site, power, and the transfer of data out of the site, avoiding mirror condensation, and achieving the excellent seeing with the observatory structures.

China is moving forward with developing the site [5]. In the (austral) summer of 2008-2009 a summer station was constructed. In the next few years, the three 0.5-m Antarctic Schmidt Telescopes (AST3) will be installed. A 1-m class pathfinder is planned to characterize the site and

Email address: agkim@lbl.gov (A. Kim)

develop the necessary technical knowhow; the intent is to eventually build a 4-10 m-class telescope.

In this paper, we explore possible supernova surveys that can be performed by these telescopes. In §2 the search and follow-up of low-redshift supernovae are discussed. In §3 the possibilities for a high-redshift search are explored. We summarize our findings in §4.

2. Low-Redshift Supernovae

A nearby sample is essential when using Type Ia supernovae as distance indicators to measure the expansion history of the universe [6]. The low-redshift anchor has strong leverage in fits of cosmological parameters. In addition, the accessibility of accurate and precise photometric and spectroscopic measurements of these high flux objects makes them an important set with which to gain a quantitative understanding of the supernova luminosity function and its sub-populations.

There are currently relatively few discovered and followed supernovae in the nearby Hubble flow at $z \approx 0.03$ – 0.1 as compared to higher redshifts, and there are several programs designed to bolster their numbers. The Nearby Supernova Factory [7], for example, targets the range $0.03 < z < 0.08$ as a sweet spot [6] where peculiar velocities are relatively small compared to the cosmological redshift and the deviation from the linear Hubble law is sensitive to the current deceleration parameter q_0 but not to individual cosmological components. At the current level of systematics, the Hubble diagram would be anchored satisfactorily by the 180 well-observed nearby supernovae we take to exist by 2011. Thus the main strength of the Dome A low-redshift supernovae is its ability to study the supernova properties themselves fulfilling the important role of mapping out systematic effects with a large sample. This includes finding subpopulations that may be relatively rare today though more common at higher redshifts. If we seek to distinguish subclasses at the 0.02 mag level in absolute magnitude, in the presence of an intrinsic scatter of 0.15 mag, this statistically requires 50 supernovae. To detect a

subclass down to 10% of the total population we would need a full set of 500 supernovae in that redshift range.

These two requirements of low enough redshift to allow thorough observation and high enough numbers to allow in-depth characterization drive the survey design. For the purposes of this note we consider a survey over $0.03 < z < 0.08$. A challenge to be faced for the low-redshift supernova discoveries is scanning the large sky area necessary to generate a significant sample. The supernova rate at $z \sim 0.1$ is 2.93×10^{-5} SNe Mpc $^{-3}h_{70}^3\text{yr}^{-1}$ [8] giving an observed rate $d^2N/(d\Omega dt) = 2.0 \delta z \text{ deg}^{-2}\text{yr}^{-1}$ at $z \sim 0.07$. The available area of sky with low airmass and Galactic dust absorption is limited at Dome A. At latitude 80.37° S, the airmass of a field with declination δ is $\text{csc}(\delta)$ to first order, and a significant fraction of sky at the south equatorial pole is covered by the Milky Way.

The useful sky available during the Antarctic winter at differing Galactic extinction can be determined using the dust maps of Schlegel, Finkbeiner, and Davis (1998) [9]. For $E(B-V) < 0.05$ over the winter, the available sky area ranges from 1600–2900 deg 2 with airmass $\chi < 1.5$ that expands to 2900–4400 deg 2 with $\chi < 2$. Extending to $0.05 < E(B-V) < 0.2$ further increases the total sky area to 7300–7800 deg 2 . For the purposes of this paper we adopt exposure times for two 4000 deg 2 areas, one with $E(B-V) = 0.05$ and the other with $E(B-V) = 0.2$. In three months 100–200 new supernova explosions are expected from $0.03 < z < 0.08$.

AST3 is comprised of three 0.5-m telescopes each equipped with an optical imager with a 4.5 deg 2 field of view with 1.0" pixels with readout much shorter than integration times. The 4000–8000 deg 2 is covered with 890–1780 pointings. The supernovae are sparse with less than one active (within two months of explosion) target per imager footprint on average.

In the following calculations we use the updated supernova template spectral time series of Hsiao et al. (2007) [10] with the mean SN Ia absolute B magnitude of $-19.46 + 5 \log(h/0.6)$ found by Richardson et al. (2002) [11], where h is the Hub-

ble constant in units of 100 km/s/Mpc.

We assume an 80% system throughput for imaging and 60% for spectroscopy. The optical to NIR sky brightness is taken to be that of CFHT at full moon, as is atmospheric absorption, since Dome A has similar sky to temperate sites at these wavelengths. The sky brightness from 2.27–2.45 μm is taken to be 100 $\mu\text{Jy}/\text{arcsec}^2$, the value measured at Dome C [4]. A seeing of $0.3'' (\lambda/0.5\mu\text{m})^{-0.2}$ added quadratically with the diffraction limit and pixelization yields the effective PSF used for 1 FWHM aperture photometry. For the case of AST3 the effective point spread function is dominated by the undersampled pixels. Supernova signal-to-noises and exposure times are calculated with SNAPsim, a simulation package of astronomical observations developed by the Supernova Acceleration Probe collaboration [12].

The requirement for the early discovery of supernovae is given as $S/N = 5$ five rest-frame days after explosion in the Hsiao et al. (2007) [10] model. Figure 1 shows the required exposure times for fields with $E(B - V) = 0.05$ and $E(B - V) = 0.2$. For a goal of $z_{\text{max}} = 0.08$, the required times with the wide (0.4-0.65 μm) filter are 60 and 150 seconds while the narrower Sloan bands require longer exposures. A 0.5-m class telescope, even if equipped with severely undersampled pixels, can provide sufficient signal-to-noise for early discovery of supernovae at low redshift. Covering the 8000 deg^2 takes ~ 52 hours of exposure plus overhead. If 16 of 24 hours are available for integration time, then it would take the three telescopes together a little over a day to observe the 8000 deg^2 , enabling a 1-day search cadence. Figure 2 shows how the required exposure times are greatly reduced if the discovery phase is relaxed to ten restframe days after explosion.

As an overall requirement for the light curve we adopt a $S/N = 25$ at peak brightness in each band, used to calculate accurate colors. The needed exposure times for the Sloan bands are shown in Figure 3. The per-band exposure times are between those necessary for five- and ten-day post-explosion discovery. Meeting the requirements in g , r , and i requires 145 s and 260 s inte-

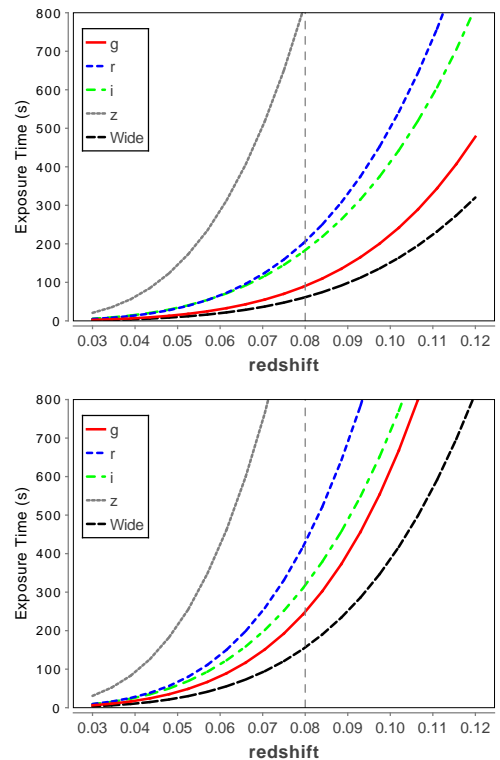


Figure 1: The exposure times required to obtain $S/N = 5$ five days after explosion for a canonical supernova at AST3 using the Sloan g , r , i , z filters and a wide filter extending from 0.4-0.65 μm . The figure on the left corresponds to a Galactic extinction of $E(B - V) = 0.05$ and the right to $E(B - V) = 0.2$.

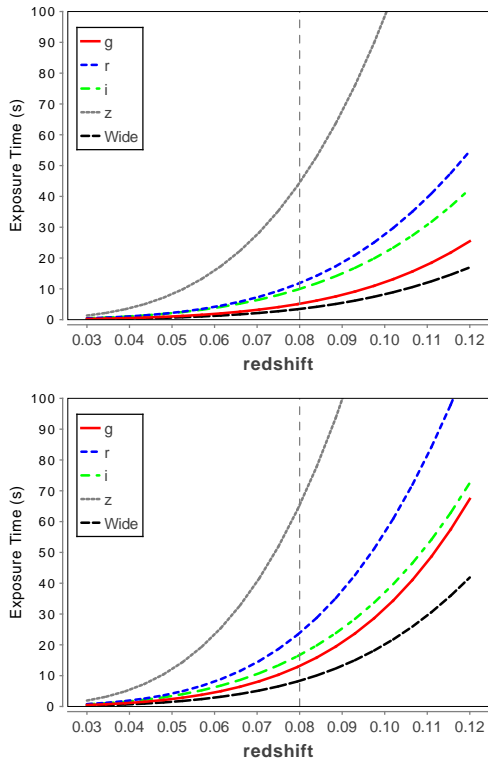


Figure 2: The exposure times required to obtain $S/N = 5$ ten days after explosion for a canonical supernova at AST3 using the Sloan g , r , i , z filters and a wide filter extending from $0.4\text{-}0.65\ \mu\text{m}$. The figure on the left corresponds to a Galactic extinction of $E(B - V) = 0.05$ and the right to $E(B - V) = 0.2$. Note that these plots have different ordinate ranges compared to those in Figure 1.

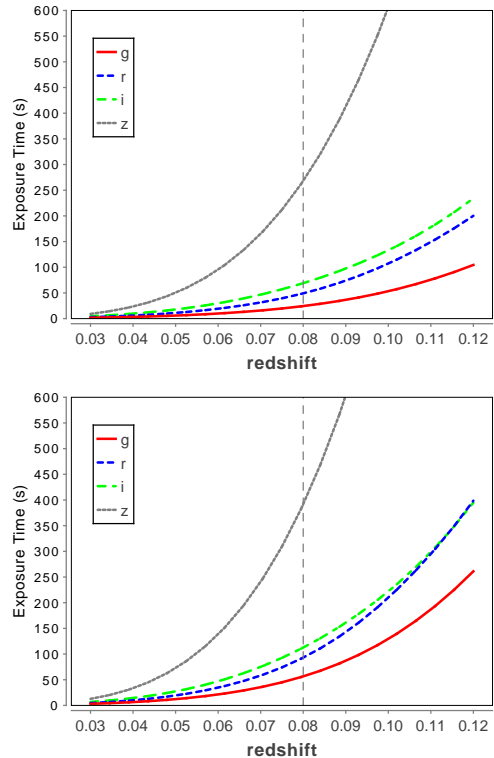


Figure 3: The exposure time required to obtain $S/N = 25$ at maximum light for a canonical supernova at AST3 in each of the Sloan g , r , i , and z filters. The figure on the left corresponds to a Galactic extinction of $E(B - V) = 0.05$ and the right to $E(B - V) = 0.2$.

grations for $E(B - V) = 0.05$ and 0.2 respectively. With the three telescopes used in a rolling search, the light curves could be sampled every 36 hours. Although most of the images will not have an active supernova such a survey requires no active exposure time nor telescope pointing decisions so it runs passively with off-line data analysis. (Moreover it would pick up other transients and build deep images of the sky.)

The 1-m pathfinder telescope can be used for spectroscopic followup. We consider an integral-field-unit spectrograph (IFU) that critically samples the $0.3''$ seeing. Its field of view is large enough to cover the supernova and several field sources needed for calibration. The spectrograph covers the full optical spectrum from $0.35 < \lambda < 1\ \mu\text{m}$ with resolution $R \gg 75$ while not being detector-noise dominated. (An $R \sim 75$ is a minimum for supernovae while a higher resolu-

tion is important for site testing.) We examine a peak-brightness exposure time requirement of $S/N = 25$ in a $\lambda/\delta\lambda = 150$ bin at rest-frame 0.443 and 0.642 μm ; this is the level of accuracy to detect heterogeneity in the spectral line ratios found by Bailey et al. (2009) [13] that calibrate supernova distances beyond standard accuracies. Exposure times as a function of redshift are shown in Figure 4. Supernovae at $z = 0.08$ in low-extinction fields require ~ 150 s exposure times and the high-extinction fields need ~ 250 s. Observing 200 supernovae with these exposure times requires ~ 11.1 hours of integration time, short enough to allow daily spectro-photometric sampling with the fixed exposure time. In a more realistic implementation, exposure times would be tuned to the actual seeing, targeted signal-to-noise, and magnitude at the date of observation, which may be brighter or fainter than our adopted number depending on supernova redshift and phase.

Daily spectro-photometric spectra can be integrated to produce light curves in synthetic photometric bands. Figure 5 shows the effective light curve signal-to-noises in [0.35–0.437], [0.437–0.552], and [0.552–0.7] μm bands for 150 s exposures of a $z = 0.08$ supernova. The exposure time, defined by the requirement to measure spectral ratios at peak brightness, generates light curves with excellent signal-to-noise throughout months of the supernova’s evolution.

The low targeted redshifts, the excellent seeing at Dome A, and the low wavelength resolution needed to measure broad spectroscopic features result in noise that is strongly source-limited for the IFU spectrograph. From a statistical standpoint this makes slitless spectroscopy a possible alternative. As an example, consider two grism channels, one from 0.35–0.5 μm and the second from 0.5–0.7 μm with $R = 75$. The wavelength ranges are tuned to give matching exposure times for the two targeted wavelengths. The exposure times necessary for the same requirements used for the IFU are shown in Figure 6; for $z = 0.08$ the time is 750 s. In the lower redshift range the exposure times are the same as with the IFU, while at higher redshift the sky contribution dominates

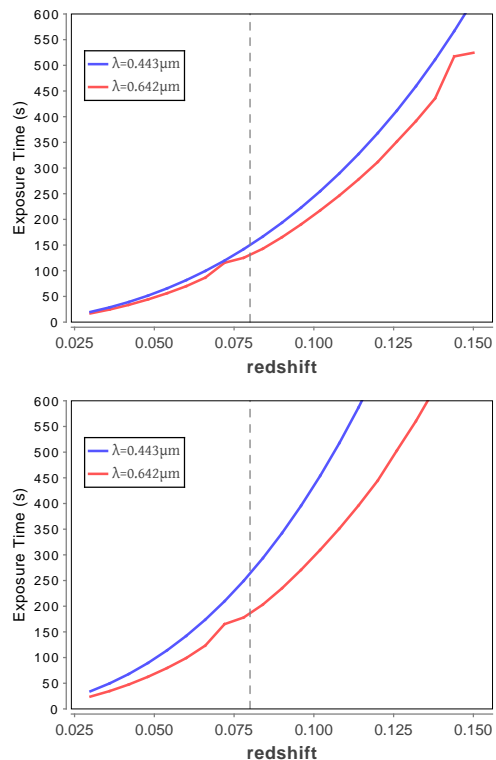


Figure 4: The exposure time required to obtain $S/N = 25$ at maximum light in a $\lambda/\delta\lambda = 150$ bin at rest-frame 0.443 and 0.642 μm for a canonical supernova using a 1-m telescope at Dome A with an integral-field-unit spectrograph. The figure on the left corresponds to a Galactic extinction of $E(B - V) = 0.05$ and the right to $E(B - V) = 0.2$.

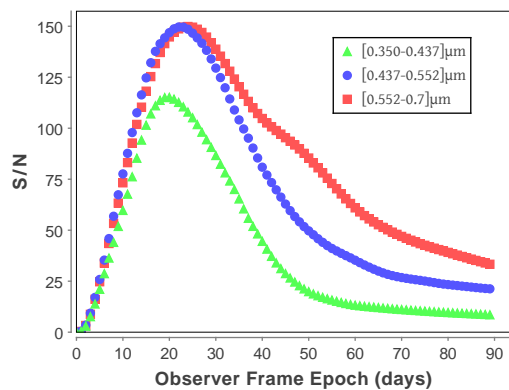


Figure 5: The signal-to-noise in three synthetic bands for a supernova at $z = 0.08$: from [0.35–0.437], [0.437–0.552], and [0.552–0.7] μm based on the conditions given in Figure 4. The light curves are based on spectra taken every 24 hours with an exposure of 150 s.

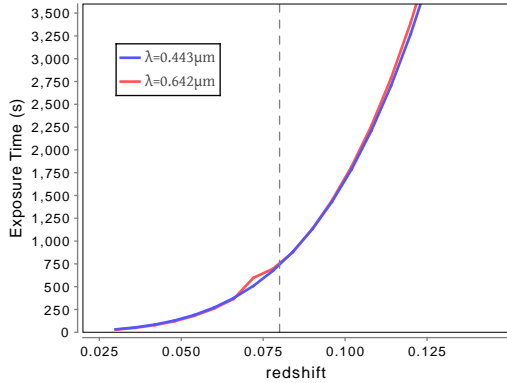


Figure 6: The exposure time required to obtain $S/N = 25$ at maximum light in a $\lambda/\delta\lambda = 150$ bin at rest-frame 0.443 and 0.642 μm for a canonical supernova using a 1-m telescope at Dome A with slitless spectroscopy split into 0.35–0.5 μm and 0.5–0.7 μm channels for $E(B-V) = 0.05$.

and exposure times increase. Slitless spectroscopy also requires longer exposures at supernova phases off peak brightness, where again the sky is the dominant background.

A wide-field slitless spectroscopic camera with a cadenced survey can generate spectroscopic time-series of all the supernovae and other bright transients in the field without the need for triggering. This deterministic survey requires no human intervention during data collection, and thus is attractive for a site such as Dome A. Synthetic photometry can be produced from the spectrum. Figure 7 shows the signal-to-noise over daily-sampled synthetic light curves obtained for a $z = 0.08$, $E(B-V) = 0.05$ supernova with a 750 s integration. Given the respective exposure times set by the requirement at peak brightness, slitless spectroscopy is qualitatively similar to the IFU (Figure 5) except at early and late phases when the supernova is faint. Slitless spectroscopy is less effective in detecting possible signatures of SN Ia heterogeneity at early and plateau phases [14, 15]. Such a focal plane faces a huge cost and technological hurdles considering the number of pixels needed for critical sampling; an imager with 0.15" pixels requires 0.578 Gpix to cover one square degree.

Another issue of interest concerns supernova

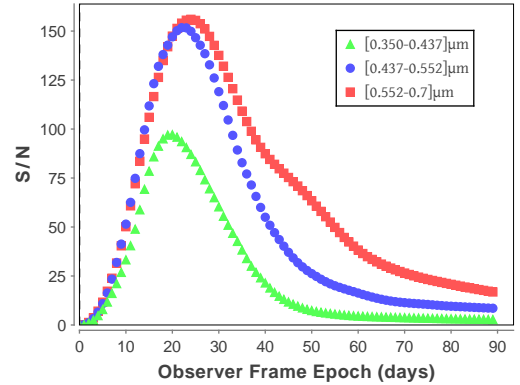


Figure 7: The signal-to-noise in three synthetic bands for a supernova at $z = 0.08$: from [0.35–0.437], [0.437–0.552], and [0.552–0.7] μm based on the conditions given in Figure 6. The light curves are based on spectra taken every 24 hours with an exposure of 750 s.

observations in the near-infrared. Supernova J and H peak magnitudes without extinction or light-curve shape correction are found to have similar RMS (~ 0.15) as those of corrected optical magnitudes [16, 17]. This smaller intrinsic dispersion in the infrared is predicted by Kasen (2006) [18]. Dust absorption uncertainties are significantly reduced as well. Expanding the set of supernovae with NIR wavelengths can help establish whether the near-infrared provides a viable alternative way to measure distances.

We assume that the 1-m telescope optics is diffraction-limited; at infrared wavelengths the instrument is an important contributor to the PSF. The exposure times to give $S/N = 25$ at peak brightness in infrared bands are shown in Figure 8. The exposure times needed to get both J and H bands together at $z = 0.08$ is ~ 120 s, similar to the time needed for spectroscopy. K band by itself would require ~ 200 s whereas K_{dark} , with its low sky emission, requires 125 s.

To summarize, the telescopes already planned for Dome A can execute a viable self-contained supernova survey. For example, data from a wide-field cadenced multi-band survey with AST3 can be processed locally to discover transients and use color and rise-time information to identify SNe Ia in the desired redshift range. The 1-m telescope is triggered for targeted follow-up using a cam-

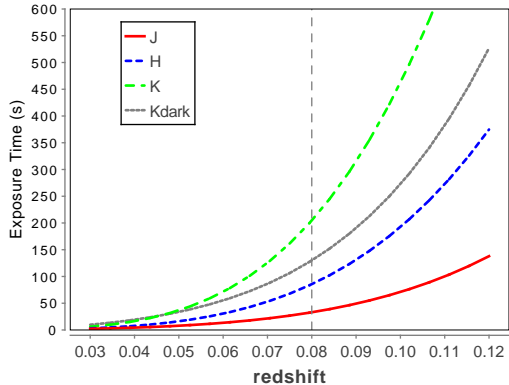


Figure 8: The exposure time required to obtain $S/N = 25$ at maximum light for a canonical supernova using a 1-m telescope at Dome A with infrared bands J , H , K , and K_{dark} . The figure corresponds to a Galactic extinction of $E(B - V) = 0.05$; exposure times are insensitive to Galactic dust at these red wavelengths.

era capable of simultaneous observations of optical spectroscopy and infrared photometry of the same field, via a dichroic. The target is confirmed as SN Ia with the spectral data and reobserved daily for the rest of the winter. Deep references are taken early in the next observing cycle when the 1-m is undersubscribed with a small list of live SN candidates. With co-located discovery and followup, non-interactive triggering and typing software that control telescope activities eliminate the need for live large data transfer out of Dome A. The full dataset can be physically retrieved for a posteriori precision reprocessing.

Such instrumentation is also appropriate for the primary goal of site characterization, in its capability to measure the seeing distribution and wavelength-dependent sky emission out to $2.5 \mu\text{m}$. For completeness, additional channels for the 1-m telescope can provide concurrent observation of an independent piece of sky with optical imaging and infrared spectroscopy. The optical imaging provides important PSF monitoring for the IFU data reduction.

3. High-redshift Supernovae

Only a few dozen high redshift ($z \gtrsim 1$) supernovae are likely to exist on the Hubble diagram

for the next several years. With sufficiently accurate observations these play important roles by providing the potential for new discoveries and further constraining dark-energy parameters [19]. A large-aperture telescope at Dome A can serve three useful purposes: measuring lightcurves for a large sample of $z \sim 1.5$ supernovae, obtaining good signal-to-noise photometry of high-redshift supernovae for discovery and triggering follow-up at other observatories, and exploring a small sample of $z \sim 2.8$ supernovae through the Antarctic “window” of the K_{dark} band.

The ~ 5 month night available for red to NIR observations at Dome A limits the coverage of the time-dilated light curves of high redshift supernovae. A demanding light-curve requirement targets measurements of the plateau phase so the period of two restframe months starting from explosion takes 5 observer months for a $z = 1.5$ supernova. This means that only objects that explode at the beginning of the winter can have a full light curve, although the partial light curves would have much more detailed coverage than usual. If the requirement were relaxed to obtain only the fall in magnitude from peak to 15 days after maximum Δm_{15} , an important parameter correlated with absolute magnitude [20], this can be determined with one rest-frame month of data (pre-max data is essential to constrain the date of maximum). Such a survey could yield two and a half months worth of $z = 1.5$ supernovae with a measurement of Δm_{15} but no information tied to homogeneity and heterogeneity at later epochs. The size of the imager field-of-view could be chosen to ensure that sufficient numbers of supernovae explode in the narrow time window. The supernova rates at $z \sim 0.8$ give an expected $36 \text{ yr}^{-1} \text{ deg}^{-2}$ per 0.1 redshift bin; rates at $z \sim 1.5$ have $1\text{-}\sigma$ uncertainties that range over a factor of five from $8\text{--}44 \text{ yr}^{-1} \text{ deg}^{-2}$ per 0.1 redshift bin, and rates are observationally unconstrained beyond $z = 1.7$ [21, 22]. As mentioned, lightcurves could be completed by feeding to mid-latitude telescopes.

Obtaining large numbers of $z > 0.8$ supernovae requires a small survey solid angle compared to the low-redshift search, so we can select a search

field with $\chi < 1.5$ airmass and $E(B-V) \sim 0$. Figure 9 shows for a range of redshifts the exposure times needed to get an early discovery of $S/N = 5$ five and ten restframe days after explosion in different bands with an 8-m telescope. With the high sky background, a small 10^{-4} flatfield uncertainty contributes non-negligibly to the overall error budget. The Z filter would be used with a thick fully-depleted CCD or HgCdTe whereas the infrared filters would be used with a HgCdTe detector. Hours of integration time are necessary to detect objects 5-days after explosion out to $z \sim 2$ in standard bands while comparable exposures in K_{dark} can access supernovae out to $z = 3$ and beyond (if there are indeed SNe Ia at these extreme redshifts). Discovery 10 days after explosion requires less than an hour in all bands out to $z = 2.5$ and tens of minutes in K_{dark} out to $z = 3$. In this sky-background-noise dominated seeing-limited regime, the exposure times scale as D^{-2} where D is the primary mirror diameter.

The faint sky in K_{dark} also offers an interesting window in which we can observe the SiII feature that defines the SN Ia class. Figure 10 shows that half-hour exposures are needed to get $S/N = 5$ in a $\lambda/\delta\lambda = 150$ element for the restframe $0.615 \mu\text{m}$ feature at peak brightness. Dome A thus provides an option for the typing of $2.75 < z < 2.95$ SNe Ia. Typing at lower redshifts is restricted as the supernova spectrum is relatively featureless at longer wavelengths.

Depending on the requirements of the survey, high-redshift supernova observations from Dome A can provide a complete dataset for cosmology, or play an important role in a larger program.

4. Conclusions

We have considered how several telescopes planned for Dome A Antarctica can be used to deliver SNe Ia science. The first set of telescopes, AST3 and a 1-m pathfinder, can produce a photometric search and spectro-photometric survey for $z < 0.08$ supernovae over an 8000 deg^2 region of sky with low airmass and Galactic-dust absorption. Depending on the goals of the survey, an instrument using slitless spectroscopy can provide a

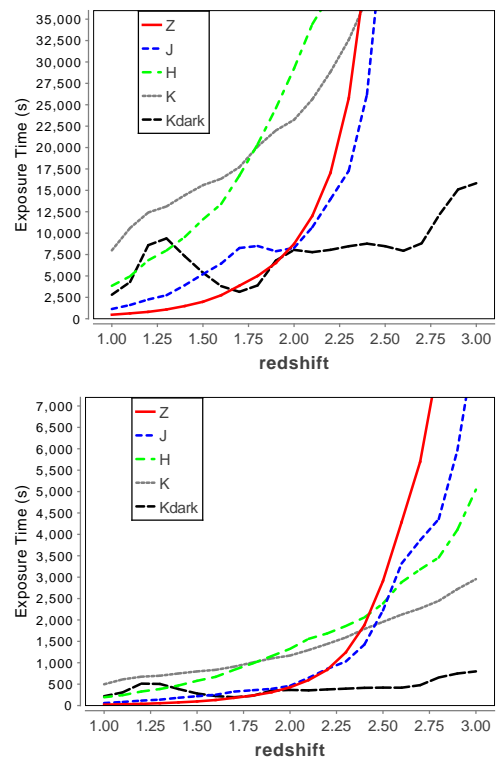


Figure 9: The exposure times required to obtain $S/N = 5$ five restframe days (left) and ten restframe days (right) after explosion for a canonical supernova using an 8-m telescope at Dome A. Note the change in scale between the two plots.

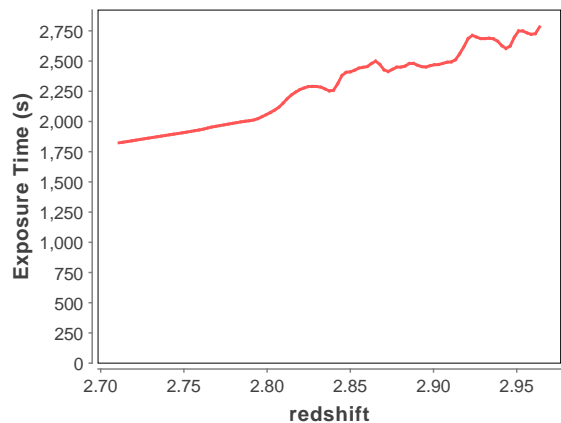


Figure 10: The exposure time required to type a canonical supernova using an 8-m telescope at Dome A, with $S/N = 5$ in a $\lambda/\delta\lambda = 150$ element for the restframe $0.615 \mu\text{m}$ SiII feature. The restricted redshift range corresponds to when the line is within the K_{dark} window.

spectroscopic time series for all bright transients in the field. However, in this case the fine pixel sampling necessary to minimize sky background and the large survey solid angles lead to enormous numbers of detector pixels.

A next-generation large aperture telescope can take advantage of the excellent seeing and the K_{dark} observing window to discover supernovae out to $z \sim 3$ and provide spectroscopic typing in a specific redshift window.

On-site analysis and telescope control reduce communication needs out of Dome A. However, the more improvement in telemetry, the more that Antarctic advantages can be used in conjunction with transient surveys occurring elsewhere in the world. Dome A discoveries can be promptly announced for observations at other observatories, and external discoveries can be followed at Dome A.

More information on site performance would enable better treatment beyond several simplifying assumptions in our calculations. We did not include host-galaxy background nor host-galaxy extinction. Our calculations are based on the fixed median seeing and not the full distribution (which can drop to 0.1"). We don't simulate the full range of SNe Ia but base our calculations on an average supernova. Exposure time estimates are based on $z = 0.08$, the high end of the targeted redshift range. We do not offer precise numbers on how far into twilight supernova observations are possible, i.e. the number of hours per night (we assume 16 hours) and the fraction of the year (we assume five months) that can be spent on the survey. Patterns of suspended observations due to weather are not considered. As more information on the site is collected, we can add more realism into our projections. Nevertheless, these first calculations show that interesting SN Ia science can be done at Dome A.

A number of other science drivers are possible as well. Mapping the peculiar velocity field at $z < 0.03$ using SNe Ia is an interesting probe of cosmology [23, 24]. With a SNe Ia rate of $\sim 0.006 \text{ deg}^{-2}\text{yr}^{-1}$, around ten years are required to build significant statistics in the restricted field available at Dome A.

Core-collapse supernovae, in particular Type IIP's, are of interest for cosmology [25, 26, 27]. Exposure times can be tuned to discover these fainter objects and the continuous observing allows monitoring for the UV shock breakout [28]. The late-time spectroscopy needed to determine velocities of the ejecta to standardize them as distance indicators does limit the time window that these supernovae can be discovered and followed at Dome A.

We have not considered the possibility of using adaptive optics at Dome A, although the greater isoplanatic angle and coherence time make this of interest. Such a capability can aid in supernova typing, but it is uncertain how it can achieve precision photometry of point sources on top of an underlying host galaxy over a large field of view.

Finally, the interest in an instrument that provides simultaneous optical IFU spectroscopy and NIR imaging of the same field is not unique to the site. Such a camera lessens the need for multi-telescope coordination in building a large set of pan-chromatic supernova data.

There remain considerable areas of interest to explore in Antarctic astronomy, supernova surveys, and their intersection. This article has presented a first look at some of the prospects and issues. With the ongoing development at Dome A and the near-term installation of wide-field and 1-m class telescopes, these topics are worth pursuing further.

5. Acknowledgements

This work was supported by the Director, Office of Science, Office of High Energy Physics, of the U.S. Department of Energy under Contract No. DE-AC02-05CH11231 and DE-AC02-07CH11359. LW is supported partially by an NSF grant AST 0708873.

- [1] L. Wang et al., Astronomy on Antarctic Plateau, *Astro2010: The Astronomy and Astrophysics Decadal Survey*, Vol. 2010 of Astronomy, 2009, pp. 308.
- [2] W. Saunders et al, *PASP*, 121, 2009, 976–992.
- [3] Phillips, A., Burton, M. G., Ashley, M. C. B., Storey, J. W. V., Lloyd, J. P., Harper, D. A., & Bally, J. 1999, *ApJ*, 527, 1009

- [4] M. G. Burton et al., *Publications of the Astronomical Society of Australia* 22, 2005, 199–235.
- [5] H. Yang et al., *PASP*, 121, 2009, 174–184.
- [6] E. V. Linder, *Phys. Rev. D*, 74 (10), 2006, 103518.
- [7] G. Aldering et al., in: J. A. Tyson & S. Wolff (Ed.), *Society of Photo-Optical Instrumentation Engineers (SPIE) Conference Series*, Vol. 4836 of *Society of Photo-Optical Instrumentation Engineers (SPIE) Conference Series*, 2002, pp. 61–72.
- [8] B. Dilday et al., *ApJ*, 682, 2008, 262–282.
- [9] D. J. Schlegel, D. P. Finkbeiner, M. Davis, *ApJ*, 500, 1998, 525.
- [10] E. Y. Hsiao et al., *ApJ*, 663, 2007, 1187–1200.
- [11] D. Richardson, D. Branch, D. Casebeer, J. Millard, R. C. Thomas, E. Baron, *AJ*, 123, 2002, 745–752.
- [12] G. Aldering et al., in: A. M. Dressler (Ed.), *Society of Photo-Optical Instrumentation Engineers (SPIE) Conference Series*, Vol. 4835 of *Society of Photo-Optical Instrumentation Engineers (SPIE) Conference Series*, 2002, pp. 146–157.
- [13] S. Bailey et al., *A&A*, 500, 2009, L17–L20.
- [14] M. Strovink, *ApJ*, 671, 2007, 1084–1097.
- [15] P. Höflich, C. Gerardy, E. Linder, et al., in: D. Alloin & W. Gieren (Ed.), *Stellar Candles for the Extragalactic Distance Scale*, Vol. 635 of *Lecture Notes in Physics*, Berlin Springer Verlag, 2003, pp. 203–227.
- [16] K. Krisciunas, M. M. Phillips, N. B. Suntzeff, *ApJ*, 602, 2004, L81–L84.
- [17] W. M. Wood-Vasey et al., *ApJ*, 689, 2008, 377–390.
- [18] D. Kasen, *ApJ*, 649, 2006, 939–953.
- [19] E. V. Linder, D. Huterer, *Phys. Rev. D*, 67 (8), 2003, 081303.
- [20] M. M. Phillips, *ApJ*, 413, 1993, L105–L108.
- [21] N. Kuznetsova et al., *ApJ*, 673, 2008, 981–998.
- [22] T. Dahlen, L. Strolger, A. G. Riess, *ApJ*, 681, 2008, 462–469.
- [23] A. G. Riess, M. Davis, J. Baker, R. P. Kirshner, *ApJ*, 488, 1997, L1.
- [24] L. Wang, *ArXiv e-prints arXiv:0705.0368*.
- [25] P. Nugent et al., *ApJ*, 645, 2006, 841–850.
- [26] D. Poznanski et al., *ApJ* 694, 2009, 1067–1079.
- [27] M. I. Jones et al., *ApJ*, 696, 2009, 1176–1194.
- [28] R. M. Quimby, J. C. Wheeler, P. Höflich, C. W. Akерlof, P. J. Brown, E. S. Rykoff, *ApJ*, 666, 2007, 1093–1107.